



34 nm-wavelength-tunable picosecond $\text{Ho}^{3+}/\text{Pr}^{3+}$ -codoped ZBLAN fiber laser

CHEN WEI,^{1,*} HONGXIA SHI,¹ HONGYU LUO,¹ HAN ZHANG,² YANJIA LYU,¹ AND YONG LIU¹

¹State Key Laboratory of Electronic Thin Films and Integrated Devices, School of Optoelectronic Information, University of Electronic Science and Technology of China (UESTC), Chengdu 610054, China

²School of Electrical Engineering Information, Sichuan University, Chengdu 610065, China
*cwei@uestc.edu.cn

Abstract: We propose and demonstrate a broadly wavelength-tunable mode-locked $\text{Ho}^{3+}/\text{Pr}^{3+}$ -codoped ZBLAN fiber laser operating in the 3 μm mid-infrared spectral region based on a semiconductor saturable absorber mirror. Wavelength selection is realized by rotating a plane ruled grating. The fiber laser exhibits stable continuous-wave mode-locking operation over a wide wavelength tuning range of 34 nm (2842.2 nm~2876.2 nm), with a 10.17 MHz repetition rate and 22 ps pulse duration. Stable mode-locked pulses can be maintained until the launched pump power of 1.25 W. Maximum average output power of 127.7 mW and the corresponding pulse energy of 12.56 nJ are achieved. To the best of our knowledge, this is the first demonstration of a wavelength-tunable mode-locked fiber laser operating in the 3 μm spectral region. Such simple, robust, and versatile mid-infrared picosecond laser source can find various applications in laser surgery, spectroscopy, and nonlinear frequency conversion.

© 2017 Optical Society of America

OCIS codes: (140.3510) Lasers, fiber; (140.3600) Lasers, tunable; (140.4050) Mode-locked lasers; (140.3070) Infrared and far-infrared lasers.

References and links

1. F. K. Tittel, D. Richter, and A. Fried, *Solid-State Mid-Infrared Laser Sources*, (Springer, 2003), Chap. 11.
2. K. Ke, C. Xia, M. N. Islam, M. J. Welsh, and M. J. Freeman, "Mid-infrared absorption spectroscopy and differential damage in vitro between lipids and proteins by an all-fiber-integrated supercontinuum laser," *Opt. Express* **17**(15), 12627–12640 (2009).
3. M. Vainio, M. Merimaa, and L. Halonen, "Frequency-comb-referenced molecular spectroscopy in the mid-infrared region," *Opt. Lett.* **36**(21), 4122–4124 (2011).
4. A. Godard, "Infrared (2–12 μm) solid-state laser sources: a review," *C. R. Phys.* **8**(10), 1100–1128 (2007).
5. M. Pollaun and S. D. Jackson, *Mid-Infrared Coherent Sources and Applications*, (Springer, 2008).
6. P. Werle, F. Slemr, K. Maurer, R. Kormann, R. Mucke, and B. Janker, "Near- and mid-infrared laser-optical sensors for gas analysis," *Opt. Lasers Eng.* **37**(2–3), 101–114 (2002).
7. X. Zhu and R. Jain, "Compact 2 W wavelength-tunable Er:ZBLAN mid-infrared fiber laser," *Opt. Lett.* **32**(16), 2381–2383 (2007).
8. X. Zhu and R. Jain, "Watt-level 100-nm tunable 3 μm fiber laser," *IEEE Photonics Technol. Lett.* **20**(2), 156–158 (2008).
9. S. Tokita, M. Hirokane, M. Murakami, S. Shimizu, M. Hashida, and S. Sakabe, "Stable 10 W Er:ZBLAN fiber laser operating at 2.71–2.88 μm ," *Opt. Lett.* **35**(23), 3943–3945 (2010).
10. L. Wetenkamp, Ch. Frerichs, G. F. West, and H. Tobben, "Efficient CW operation of tunable fluorozirconate fibre lasers at wavelengths pumpable with semiconductor laser diodes," *J. Non-Cryst. Solids* **140**, 19–24 (1992).
11. L. Wetenkamp, "Efficient CW operation of a 2.9 μm Ho^{3+} -doped fluorozirconate fiber laser pumped at 640 nm," *Electron. Lett.* **26**(13), 883–884 (1990).
12. D. Hudson, E. Magi, L. Gomes, and S. D. Jackson, "1 W diode-pumped tunable Ho^{3+} , Pr^{3+} -doped fluoride glass fiber laser," *Electron. Lett.* **47**(17), 985–986 (2011).
13. J. Li, D. D. Hudson, and S. D. Jackson, "Tuned cascade laser," *IEEE Photonics Technol. Lett.* **24**(14), 1215–1217 (2012).
14. S. Crawford, D. D. Hudson, and S. D. Jackson, "High-power broadly tunable 3- μm fiber laser for the measurement of optical fiber loss," *IEEE Photonics J.* **7**(3), 1–9 (2015).
15. M. R. Majewski and S. D. Jackson, "Tunable dysprosium laser," *Opt. Lett.* **41**(19), 4496–4498 (2016).

16. O. Henderson-Sapir, S. D. Jackson, and D. J. Ottaway, "Versatile and widely tunable mid-infrared erbium doped ZBLAN fiber laser," *Opt. Lett.* **41**(7), 1676–1679 (2016).
17. G. Zhu, L. Geng, X. Zhu, L. Li, Q. Chen, R. A. Norwood, T. Manzur, and N. Peyghambarian, "Towards ten-watt-level 3-5 μm Raman lasers using tellurite fiber," *Opt. Express* **23**(6), 7559–7573 (2015).
18. C. Wei, X. Zhu, R. A. Norwood, F. Song, and N. Peyghambarian, "Numerical investigation on high power mid-infrared supercontinuum fiber lasers pumped at 3 μm ," *Opt. Express* **21**(24), 29488–29504 (2013).
19. M. Skorzczakowski, J. Swiderski, W. Pichola, P. Nyga, A. Zajac, M. Maciejewska, L. Galecki, J. Kasprzak, S. Gross, A. Heinrich, and T. Bragagna, "Mid-infrared Q-switched Er: YAG laser for medical applications," *Laser Phys. Lett.* **7**(7), 498–504 (2010).
20. Q. Ren, V. Venugopalan, K. Schomacker, T. F. Deutsch, T. J. Flotte, C. A. Puliafito, and R. Birngruber, "Mid-infrared laser ablation of the cornea: a comparative study," *Lasers Surg. Med.* **12**(3), 274–281 (1992).
21. H. A. Wigdor, J. T. Walsh, Jr., J. D. Featherstone, S. R. Visuri, D. Fried, and J. L. Waldvogel, "Lasers in dentistry," *Lasers Surg. Med.* **16**(2), 103–133 (1995).
22. L. I. Deckelbaum, "Cardiovascular applications of laser technology," *Lasers Surg. Med.* **15**(4), 315–341 (1994).
23. M. Gorjan, R. Petkovšek, M. Marinček, and M. Čopič, "High-power pulsed diode-pumped Er:ZBLAN fiber laser," *Opt. Lett.* **36**(10), 1923–1925 (2011).
24. Y. L. Shen, K. Huang, S. Q. Zhou, K. P. Luan, L. Yu, A. Q. Yi, G. B. Feng, and X. S. Ye, "Gain-switched 2.8 μm Er³⁺-doped double-clad ZBLAN fiber laser," *Proc. SPIE* **9543**, 95431E (2015).
25. C. Wei, H. Luo, H. Shi, Y. Lyu, H. Zhang, and Y. Liu, "Widely wavelength tunable gain-switched Er³⁺-doped ZBLAN fiber laser around 2.8 μm ," *Opt. Express* **25**(8), 8816–8827 (2017).
26. J. Li, Y. Yang, D. D. Hudson, Y. Liu, and S. D. Jackson, "A tunable Q-switched Ho³⁺-doped fluoride fiber laser," *Laser Phys. Lett.* **10**(4), 045107 (2013).
27. J. Li, H. Luo, L. Wang, B. Zhai, H. Li, and Y. Liu, "Tunable Fe²⁺:ZnSe passively Q-switched Ho³⁺-doped ZBLAN fiber laser around 3 μm ," *Opt. Express* **23**(17), 22362–22370 (2015).
28. G. Zhu, X. Zhu, K. Balakrishnan, R. A. Norwood, and N. Peyghambarian, "Fe²⁺: ZnSe and graphene Q-switched singly Ho³⁺-doped ZBLAN fiber lasers at 3 μm ," *Opt. Mater. Express* **3**(9), 1365–1377 (2013).
29. C. Wei, H. Luo, H. Zhang, C. Li, J. Xie, J. Li, and Y. Liu, "Passively Q-switched mid-infrared fluoride fiber laser around 3 μm using a tungsten disulfide (WS₂) saturable absorber," *Laser Phys. Lett.* **13**(10), 105108 (2016).
30. Z. Qin, G. Xie, H. Zhang, C. Zhao, P. Yuan, S. Wen, and L. Qian, "Black phosphorus as saturable absorber for the Q-switched Er:ZBLAN fiber laser at 2.8 μm ," *Opt. Express* **23**(19), 24713–24718 (2015).
31. C. Wei, H. Zhang, H. Shi, K. Konynenbelt, H. Luo, and Y. Liu, "Over 5W passively Q-switched mid-infrared fiber laser with a wide continuous wavelength tuning range," *IEEE Photonics Technol. Lett.* **29**(11), 881–884 (2017).
32. S. Duval, M. Bernie, V. Forti, J. Genest, M. Pichel, and R. Vallée, "Femtosecond fiber lasers reach the mid-infrared," *Optica* **2**(7), 623–626 (2015).
33. T. Hu, S. D. Jackson, and D. D. Hudson, "Ultrafast pulses from a mid-infrared fiber laser," *Opt. Lett.* **40**(18), 4226–4228 (2015).
34. J. Li, D. D. Hudson, Y. Liu, and S. D. Jackson, "Efficient 2.87 μm fiber laser passively switched using a semiconductor saturable absorber mirror," *Opt. Lett.* **37**(18), 3747–3749 (2012).
35. T. Hu, D. D. Hudson, and S. D. Jackson, "Stable, self-starting, passively mode-locked fiber ring laser of the 3 μm class," *Opt. Lett.* **39**(7), 2133–2136 (2014).
36. A. Haboucha, V. Fortin, M. Bernier, J. Genest, Y. Messaddeq, and R. Vallée, "Fiber Bragg grating stabilization of a passively mode-locked 2.8 μm Er³⁺: fluoride glass fiber laser," *Opt. Lett.* **39**(11), 3294–3297 (2014).
37. P. Tang, Z. Qin, J. Liu, C. Zhao, G. Xie, S. Wen, and L. Qian, "Watt-level passively mode-locked Er³⁺-doped ZBLAN fiber laser at 2.8 μm ," *Opt. Lett.* **40**(21), 4855–4858 (2015).
38. C. Wei, X. Zhu, R. A. Norwood, and N. Peyghambarian, "Passively continuous-wave mode-locked Er³⁺-doped ZBLAN fiber laser at 2.8 μm ," *Opt. Lett.* **37**(18), 3849–3851 (2012).
39. Z. Qin, G. Xie, C. Zhao, S. Wen, P. Yuan, and L. Qian, "Mid-infrared mode-locked pulse generation with multi-layer black phosphorus as saturable absorber," *Opt. Lett.* **41**(1), 56–59 (2016).
40. G. Zhu, X. Zhu, F. Wang, S. Xu, Y. Li, K. Balakrishnan, R. A. Norwood, and N. Peyghambarian, "Graphene mode-locked fiber laser at 2.8 μm ," *IEEE Photonics Technol. Lett.* **28**(1), 7–10 (2016).
41. J. Li, H. Luo, B. Zhai, R. Lu, Z. Guo, H. Zhang, and Y. Liu, "Black phosphorus: a two-dimension saturable absorption material for mid-infrared Q-switched and mode-locked fiber lasers," *Sci. Rep.* **6**(1), 30361 (2016).
42. X. Zhu, G. Zhu, C. Wei, L. V. Kotov, J. Wang, M. Tong, R. A. Norwood, and N. Peyghambarian, "Pulsed fluoride fiber lasers at 3 μm [Invited]," *J. Opt. Soc. Am. B* **34**(3), A15–A28 (2017).
43. V. A. Serebryakov, É. V. Boiko, N. N. Petrishchev, and A. V. Yan, "Medical applications of mid-IR lasers. Problems and prospects," *J. Opt. Technol.* **77**(1), 6–17 (2010).
44. X. Zhu and R. Jain, "Watt-level 100-nm tunable 3 μm fiber laser," *IEEE Photonics Technol. Lett.* **20**(2), 156–158 (2008).

1. Introduction

Wavelength tunable lasers emitting light around 3 μm have attracted great attention owing to their wide variety of applications in spectroscopy, laser surgery, remote sensing, missile countermeasure, frequency metrology, light detection and ranging (LIDAR), and nonlinear

mid-infrared photonics [1–6]. Compared to other types of lasers, fiber lasers feature favorable characteristics such as outstanding beam quality, good heat dissipation, high conversion efficiency, and compact structure. Efficient laser emissions at wavelengths around 3 μm were demonstrated in Er^{3+} [7–10], Ho^{3+} [11], $\text{Ho}^{3+}/\text{Pr}^{3+}$ [12–14], and Dy^{3+} [15] doped fluoride fibers. Tunable sources in both continuous-wave (CW) and pulsed operation have been successfully achieved. To date, wavelength-tunable Er^{3+} -doped ZBLAN fiber lasers operating in the CW regime with a maximum output power of 11 W (2770–2880 nm) [9] and with the broadest tuning range of 160 nm (2670–2830 nm) around 2.8 μm [10] have been demonstrated. By tuning the ${}^4\text{F}_{9/2} \rightarrow {}^4\text{I}_{9/2}$ transition, 450 nm wavelength tuning range from 3.33 μm to 3.78 μm has been reported in an Er^{3+} -doped ZBLAN fiber laser in the CW operation [16]. Besides, wavelength tuning has also been investigated in Ho^{3+} -doped and $\text{Ho}^{3+}/\text{Pr}^{3+}$ -codoped ZBLAN fibers. Maximum average output power of 7.2 W with the broadest tuning range of 150 nm (2825–2975 nm) has been achieved [14]. Recently, wavelength tunable Dy^{3+} -doped ZBLAN fiber laser with a tuning range of 400 nm from 2.95 to 3.35 μm has been demonstrated [15].

Nevertheless, ~ 3 μm wavelength tunable pulsed lasers with peak powers some orders of magnitude higher than that in the CW regime are highly demanded for nonlinear wavelength converters and medical applications, such as cardiovascular surgery, vitreoretinal surgery, and dental tissue ablation [17–22]. To achieve flexible pulses with μs - or ns- pulse duration, various approaches including gain-switching [23–25] and Q-switching [26–30] have been utilized. Utilizing a pulsed pump source, we demonstrated a wavelength widely tunable gain-switched Er^{3+} -doped ZBLAN fiber laser around 2.8 μm . The stable single-pulse gain-switched laser pulses can be tuned over 170 nm (2699 nm–2869.9 nm) for various pump power levels [25]. Very recently, we demonstrated a five-watt passively Q-switched Er^{3+} -doped ZBLAN fiber laser that could be tuned over a wavelength range of 90 nm from 2762.5 nm to 2852.5 nm [31]. Compared to gain-switched and Q-switched lasers, mode-locked lasers offer much higher peak powers and shorter pulse durations in the ps- or fs- level that are in great demand for a wide variety of applications such as mid-IR nonlinear wavelength conversion and medical surgery, where high-energy/peak power is essential, and shorter pulses are preferred. So far, many mode-locked fiber lasers operating at ~ 3 μm have been reported, mainly based on nonlinear polarization evolution (NPE) technology [32,33] or saturable absorbers such as semiconductor saturable absorber mirror (SESAM) [34–37], Fe^{2+} : ZnSe [38], and two-dimensional materials [39–41]. Femtosecond fluoride fiber lasers operating at ~ 3 μm based on nonlinear polarization evolution (NPE) with an average power of 44 mW and 206 mW were demonstrated [32,33]. However, NPE based mode-locked lasers usually require critical resonator alignment and frequent adjustment, and the optimum polarization settings can drift with temperature [42]. Incorporating a saturable absorber with suitable properties into the laser resonator is another way to achieve the stable mode-locking operation. Two-dimensional materials such as black phosphorus [39] and graphene [40] have been utilized to realize 3 μm mode-locked fiber lasers. 42 ps pulses with high output power of 613 mW at a repetition rate of 24 MHz and 18 mW at a repetition rate of 25.4 MHz were obtained, respectively. Compared to two-dimensional materials, SESAM has advantages of high stability, convenient pulse self-starting, and high optical power handling. Thanks to the recent mature semiconductor manufacturing techniques, high quality SESAM with expected absorption and modulation depth can be easily and precisely fabricated. In 2012, Li et al. reported a partially mode-locked $\text{Ho}^{3+}/\text{Pr}^{3+}$ -codoped ZBLAN fiber laser by using an InAs-based SESAM. 24 ps pulses with an average power of 132 mW at a repetition rate of 27.1 MHz were achieved [34]. Two years later, a stable CW mode-locked $\text{Ho}^{3+}/\text{Pr}^{3+}$ -codoped ZBLAN fiber laser was demonstrated by employing a transmissive InAs SESAM in a ring-cavity laser configuration. 6 ps pulses with an average output power of 69.2 mW at a repetition rate of 24.8 MHz were observed [35]. Meanwhile, by implementing a fiber Bragg grating, Haboucha et al. achieved a stable SESAM based mode-locking operation in an Er^{3+} -doped fiber laser linear cavity. 60 ps

pulses with an average power of 440 mW at a repetition rate of 51.75 MHz were obtained [36]. Tang et al. reported stable operation of a SESAM mode-locked Er^{3+} -doped ZBLAN fiber laser at a relatively large range of high pump powers and improved the output power to 1 W [37]. Unfortunately, all the mode-locked fiber lasers in the 3 μm spectral region operate at fixed wavelengths. For some practical applications in less-invasive and high-precision laser surgery (such as ophthalmology and neuro- and cardiosurgery), selective excitation, spectroscopic sensors, and nonlinear frequency conversion, wavelength tunability of mode-locked lasers are highly demanded [43,44]. Tunable mode-locked fiber lasers at $\sim 3 \mu\text{m}$ with flexible output wavelengths, high radiation intensity and relatively low pulse energy at high repetition frequency will open up new possibilities in an increasing number of applications.

In this work, we demonstrate the wavelength tuning in a $\text{Ho}^{3+}/\text{Pr}^{3+}$ -codoped ZBLAN fiber laser that is mode-locked with a SESAM. A plane ruled reflectance grating is used to provide wavelength tunability and cavity feedback. By rotating the plane ruled grating, we obtain a tuning range of 34 nm spanning from 2842.2 nm to 2876.2 nm, while keeping the laser operating in the stable CW mode-locking regime. The stable and self-starting mode-locking regime is characterized by the high optical signal-to-noise ratio (SNR) of ~ 60 dB and is maintained over several hours. This is the first demonstration, to the best of our knowledge, of the wavelength tunable mode-locked fiber laser operating around 3 μm .

2. Experimental setup

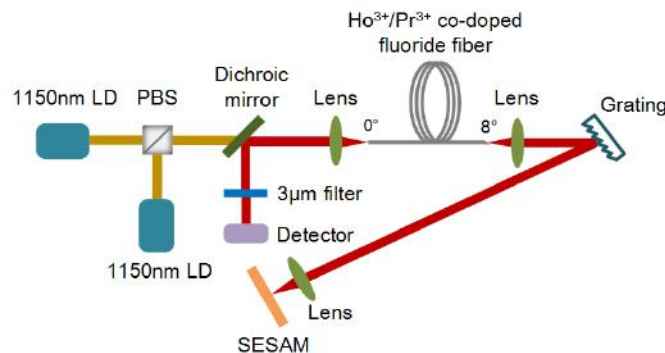


Fig. 1. Schematic diagram of the tunable passively mode-locked $\text{Ho}^{3+}/\text{Pr}^{3+}$ codoped fluoride fiber laser based on SESAM.

The schematic diagram of the wavelength tunable passively mode-locked $\text{Ho}^{3+}/\text{Pr}^{3+}$ codoped ZBLAN fiber laser using SESAM is shown in Fig. 1. The laser from two commercially available high power 1150 nm diode lasers (Eagleyard Photonics, Berlin) was coupled into the gain fiber after polarization multiplexing via a polarized beam splitter (PBS) and focused by a 1150 nm anti-reflection coated ZnSe objective lens (focal length: 6.0 mm) acting as the collimator for the light out-coupled from the gain fiber core as well. A dichroic mirror between the PBS and the ZnSe objective lens was placed at an angle of 45° with respect to the pump beam to direct the laser output. The gain fiber (Fiberlabs, Japan) was a piece of double-cladding $\text{Ho}^{3+}/\text{Pr}^{3+}$ codoped ZBLAN fiber doped with 3 mol. % Ho^{3+} ions and 0.25 mol. % Pr^{3+} ions. It has an octagonal pump core with a diameter of 125 μm and NA of 0.5 and a circular core with a diameter of 10 μm and NA of 0.2. The selected fiber length of 9.0 m could provide $>90\%$ pump absorption efficiency. In this system, the front fiber end was perpendicularly cleaved providing $\sim 4\%$ feedback and worked as the output coupler, while the rear end was angle cleaved ($\sim 10^\circ$) to eliminate the influence of the Fresnel reflection. Two anti-reflection coated ZnSe objective lenses were used to collimate and focus the emission from the angle cleaved fiber end onto the SESAM. The GaAs-based SESAM (BATOP GmbH) is designed to operate at 2800 nm with an absorbance of 12% and has a relaxation

time of 10 ps. Wavelength tuning was realized by rotating a plane ruled grating (450 lines/mm, blazed at $3.1\ \mu\text{m}$, 88~91.5% reflectivity at $2.8\sim 2.9\ \mu\text{m}$) placed in the laser resonator as shown in Fig. 1. The average power of the output laser beam was measured with a power meter (Laserpoint) after passing through an IR bandpass filter (Thorlabs, FB2750-500). An InAs detector with a response time of 2 ns was connected with a 500 MHz bandwidth digital oscilloscope to record the pulse temporal waveforms. A radio frequency (RF) spectrum analyzer (YIAI, AV4033A) was used to measure the RF spectrum of the pulses. A monochromator with a scanning resolution of 0.1 nm (Princeton instrument Acton SP2300) was utilized to measure the optical spectrum.

3. Results and discussion

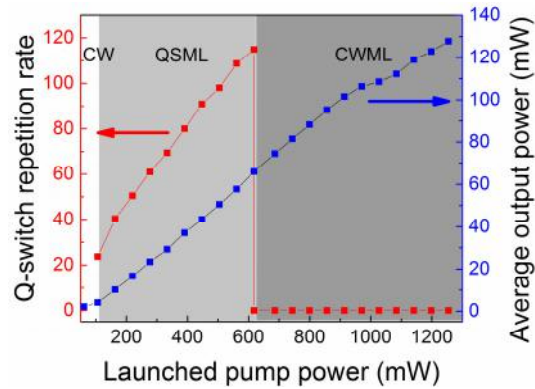


Fig. 2. Average output power and Q-switched repetition rate with respect to the launched pump power. The three operation regimes are also shown. CW: continuous-wave operation; QSML: Q-switched mode-locking operation; CWML: continuous-wave mode-locking operation.

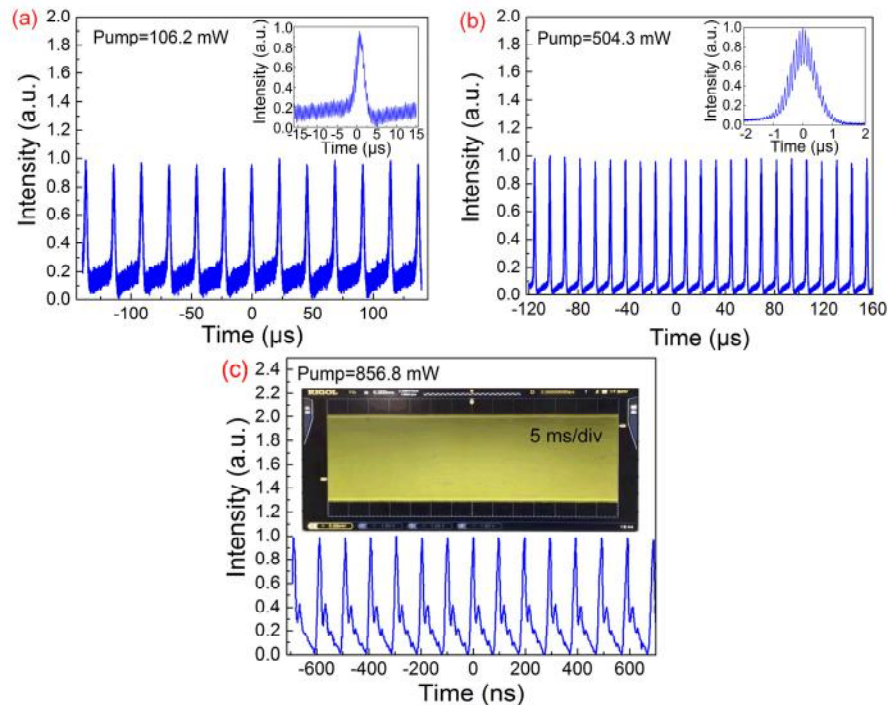


Fig. 3. Pulse trains at various launched pump powers. (a) & (b) Q-switched mode-locked pulse trains at launched pump power of (a) 106.2 mW and (b) 504.3 mW. Insets: single pulse profiles; (c) CW mode-locked pulse trains at launched pump power of 856.8 mW. Inset: CW pulse train over a long time scale (70 ms).

Figure 2 shows the output power as a function of the launched pump power. It is observed that the output power increases almost linearly with the launched pump power at a slope efficiency of 11.2%. CW operation started at the launched pump power of approximately 60.7 mW. As the launched pump power was increased to 106.2 mW, Q-switched mode-locked (QSML) pulses were generated, as shown in Fig. 3(a). The Q-switched mode-locked pulses have a large Q-switched envelope with a duration (defined as the full width at half maximum (FWHM) of the single Q-switched pulse envelope) of approximately 2.6 μs , with sharp features at a 10.17 MHz repetition rate that matched the inverse of the round trip time of the cavity. As the pump power was steadily increased to 617.9 mW, the repetition rate of the Q-switched envelope also increased from 23.7 kHz to 114.9 kHz while the pulse duration decreased from 2.6 μs to 700 ns. Figure 3(b) shows the typical QSML pulse trains at the launched pump power of 504.3 mW. The repetition rate and pulse duration were 98 kHz and 0.9 μs , respectively.

For launched pump powers higher than 617.9 mW, the laser immediately self-started to a stable CWML regime. The transition from the QSML regime to the CWML regime is highlighted in Fig. 2. The end of the light gray region, where the Q-switching repetition rate drops to zero, marks the transition point. This mode-locking operation was sustained up to 1.25 W of launched pump power and output average power of 127.7 mW was obtained. Stable mode-locking operation at 127.7 mW output power could be sustained for over 3 hours. Higher output power could be achieved by increasing the pump power, but strong CW components and multiple-pulsing tendency could not be restrained. When the launched pump power was lower than 1.25 W, no multi-pulse or harmonic mode-locking was observed. The typical mode-locked pulse train measured by the oscilloscope at the launched power of 856.8 mW is shown in Fig. 3(c). The inset of Fig. 3(c) shows the temporal pulse train in CWML regime at a scanning span of 70 ms. We can see that the laser produced mode-locked pulses at 10.17 MHz repetition rate with no amplitude variation. It is worth mentioning that a pure Q-switched operation was not found. However, if the saturable absorber was displaced slightly away from the focus of the laser beam, Q-switching was observed, in accordance with previous reports [34,38].

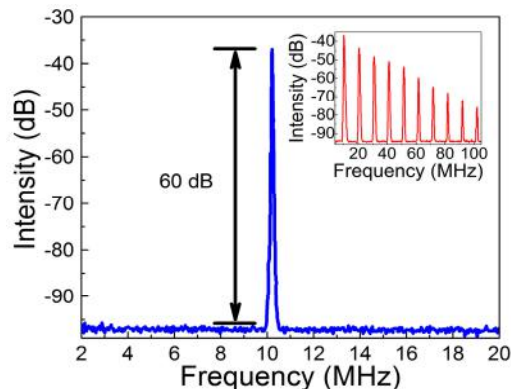


Fig. 4. RF spectrum of mode-locked pulses centered at 10.17 MHz with a SNR of 60 dB. Inset: RF spectrum over a 100 MHz range. (Launched pump power: 856.8 mW).

In order to understand the stability of the mode-locking operation, we measured the RF spectra of the pulses, as shown in Fig. 4. The fundamental beat note at 10.17 MHz measured with a resolution bandwidth of 10 kHz within a 20 MHz span, exhibited a high SNR of 60 dB. The inset of Fig. 4 shows a 100 MHz wide-span RF measurement of the pulse signal. Two RF spectra with a high SNR and the absence of any specious modulation indicate a stable single-pulse CWML operation without unwanted multiple pulsing and Q-switching modulation.

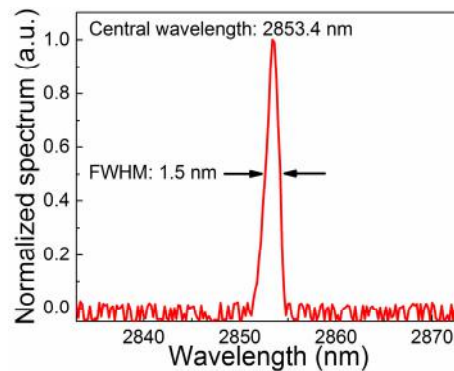


Fig. 5. Measured optical spectrum at the launched pump power of 856.8 mW.

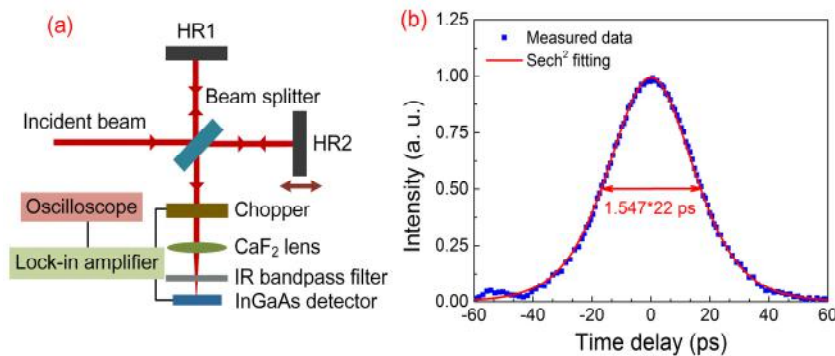


Fig. 6. (a) Schematic of the in-house autocorrelator based on two-photon absorption in an InGaAs detector; (b) the autocorrelation trace at the launched pump power of 856.8 mW. The blue circles are the measured data and the red curve represents the fitting result.

The optical spectrum was measured during the CWML regime. Figure 5 plotted the optical spectrum of the laser at the launched pump power of 856.8 mW. The spectrum has a FWHM of 1.5 nm centered at 2853.4 nm. The optical pulse duration was measured with a home-made autocorrelator, as shown in Fig. 6(a). Two-photon absorption in an InGaAs photodiode was used to detect the autocorrelation signal. To prevent residual pump light and background noise, an IR bandpass filter (center wavelength: 2750 nm, FWHM: 500 nm) was placed in front of the InGaAs detector. An optical beam chopper and lock-in amplifier were used to accurately measure the weak two-photon signal generated from the InGaAs photodiode. A digital oscilloscope was connected to the lock-in amplifier to record the autocorrelation trace. The autocorrelation trace for pulses at the launched pump power of 856.8 mW is shown in Fig. 6(b). The FWHM was calculated to be 34 ps. Thus, the mode-locked pulse duration was deduced to be 22 ps, based on a sech^2 -shaped pulse which provided the best fit to the data. The time-bandwidth product was calculated to be 1.29, which indicates that the mode-locked pulses were not transform limited. The pulse lengthening was most likely because that the pulses were chirped by dispersion in the fluoride fiber. By introducing dispersion compensating components to administrate the net dispersion, shorter mode-locked pulses are expected.

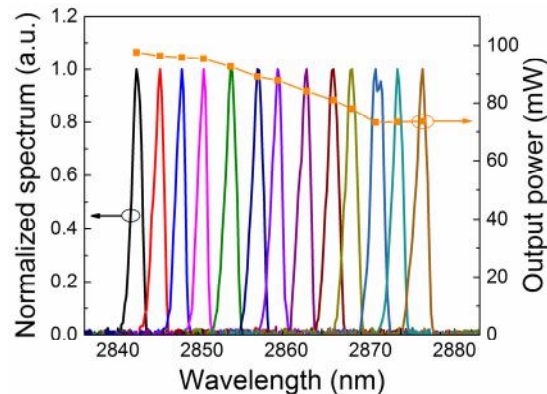


Fig. 7. Normalized spectra (left scale) together with the corresponding average output power (right scale) from the SESAM mode-locked ZBLAN fiber laser. (Launched pump power: 856.8 mW).

By rotating the plane ruled grating placed in the laser resonator, the central wavelength of the CW mode-locked pulses was continuously tuned. The wavelength could be continuously tuned at a pump power above the threshold of 617.9 mW. Considering the stability and the tuning range of the mode-locked laser, we chose a moderate pump power of 856.8 mW and investigated on the tuning characteristics. Up to 34 nm tuning range (2842.2 nm~2876.2 nm) with the output powers varies from 97.6 mW to 74.2 mW was obtained experimentally at the launched pump power of 856.8 mW. Figure 7 shows the corresponding spectra and output powers. The output spectra's FWHMs of different wavelengths vary from 1.4 nm (at 2842.2 nm) to 1.5 nm (at 2876.2 nm). No significant changes on the pulse durations (~22 ps) and repetition rates (10.17 MHz) of the mode-locked laser were observed during the whole tuning range. Wider-tuning-range mode-locking is not feasible in this oscillator. Further rotating the grating toward longer wavelengths led to the QSML operation. Stable QSML operation could be maintained with the central wavelength tuned from 2878.0 nm to 2891.4 nm (~13.4 nm). The output powers varied from 69.3 mW to 75.2 mW with the tuning wavelengths.

It is well known that in order to realize mode-locking, the following condition must be satisfied: $E_p^2 > E_{sat,L} E_{sat,A} \Delta R$, where E_p is the intra-cavity pulse energy, $E_{sat,L}$ and $E_{sat,A}$ are the saturation energies of the used gain fiber and SA, ΔR is the modulation depth of the SA. According to the low intensity spectral reflectance versus wavelength of the SESAM provided by the manufacture, the SESAM's low intensity reflectance almost linearly decreases below 90% when the wavelength comes to 2842.2 nm, which made the modulation depth ΔR too large to initiate mode-locking according to $\Delta R = A_0 - A_{ns}$ (A_0 : absorption, A_{ns} : non-saturable loss and $A_0 = 1 - R$ (R : low intensity reflectance)). As for 2876.2 nm, the cavity's gain became not enough. So the tuning range was limited in 2842.2 nm~2876.2 nm to realize stable mode-locking operation.

By replacing the SESAM with a gold mirror in the same configuration, no pulse operation could be achieved no matter how to adjust the gold mirror. The CW laser could be tuned over 52 nm from 2841.8 nm to 2894 nm by rotating the plane ruled grating. In the laser cavity, the SESAM provided both robust self-starting and strong pulse shaping mechanisms to ensure the stable mode-locking. In the future, it is worthy trying a wider-spectral-range SESAM with flatter reflection to achieve continuous wavelength tuning over the entire spectral gain bandwidth in one compact fiber laser configuration. It's worth noting that the use of an in-cavity grating limited the pulse bandwidth, and hence the peak power was limited. However, for certain applications such as nonlinear frequency conversion, not only precise wavelength adjustment but also high peak power is required. This wavelength-tunable picosecond mid-infrared fiber laser can be used as a practical seed source for further power amplification. Further boosting the output power by introducing additional amplifiers utilizing the master oscil-

lator power amplifier (MOPA) system is underway. Much higher output power and/or energy pulses can be expected by using a MOPA system to boost the pulses.

4. Conclusion

In conclusion, we have demonstrated a widely tunable mode-locked $\text{Ho}^{3+}/\text{Pr}^{3+}$ -codoped ZBLAN fiber laser at $\sim 3 \mu\text{m}$ based on SESAM with a linear cavity design. The wavelength selection was realized by rotating the plane ruled grating. In the stable single-pulse regime, the average output power of up to 127.7 mW at 10.17 MHz repetition rate was achieved, resulting in a single pulse energy of 12.56 nJ and peak power of 503.5 W. The central wavelength of the passively mode-locked laser could be tuned in a wide range of 34 nm from 2842.2 nm to 2876.2 nm. This is, to the best of our knowledge, the first wavelength tunable mode-locked fiber laser in the 3 μm MIR spectral region. Such flexible fiber laser has the advantage of large tuning range at the 3 μm band and may find versatile applications in laser surgery, spectroscopy, and mid-infrared supercontinuum generation and mid-infrared pump-probe experiments.

Funding

National Natural Science Foundation of China (NSFC) (61435003, 61505024, 61421002); Science and Technology Project of Sichuan Province (2016JY0102); Science and Technology Innovation Young Talent Project of Sichuan Province (2016RZ0073).